Microstructure-based 3D modelling of diffusivity in sound and cracked cement paste

Mazaheripour, Hadi; Faria, Rui; Azenha, Miguel; Ye, Guang; Schlangen, Erik

Publication date
2018

Document Version
Final published version

Published in
Proceedings of the Symposium on Concrete Modelling

Citation (APA)
Mazaheripour, H., Faria, R., Azenha, M., Ye, G., & Schlangen, E. (2018). Microstructure-based 3D modelling of diffusivity in sound and cracked cement paste. In E. Schlangen, G. de Schutter, B. Šavija, H. Zhang, & C. Romero Rodriguez (Eds.), *Proceedings of the Symposium on Concrete Modelling: CONMOD2018 27-30 August 2018 – Delft, Netherlands* (Vol. PRO 127, pp. 321-332). (Rilem proceedings; No. PRO 127). Rilem.

Symposium on Concrete Modelling (CONMOD2018) –
27-30 August 2018 – Delft, Netherlands

MICROSTRUCTURE-BASED 3D MODELLING OF DIFFUSIVITY IN SOUND AND CRACKED CEMENT PASTE

Hadi Mazaheripour [(1)], Rui Faria [(2)], Miguel Azenha [(2)], Guang Ye [(3)], Erik Schlangen[(3)]

(1) CONSTRUCT, Faculty of Engineering, University of Porto (FEUP), Portugal

(2) ISISE, University of Minho, Portugal

(3) Microlab, Delft University of Technology (TU Delft), Netherlands

Abstract

Exposing reinforced concrete (RC) structures to aggressive environmental conditions is one of the main reasons that may limit their service life. Diffusion of chloride ions through concrete cover is one of the most damaging environmental actions, since it may cause corrosion of steel reinforcement. Therefore, modelling this phenomenon allows supporting a better durability assessment of RC structures. In the present study, a modelling strategy considering a 3D cement paste microstructure, which is obtained using HYMOSTRUC3D software, is adopted to compute the diffusion process in saturated sound and cracked cement pastes. The diffusion process is calculated as a statistical result of random walkers (representing ionic species) through the porosity of the cement paste microstructure. The simulation is implemented using a random walk algorithm (RWA), which is compatible to be used in sound and cracked cement paste microstructures. Additionally, the proposed modelling strategy aims to establish a relation between the diffusion coefficient of cement paste and the level of tensile damage in the microstructure, which is obtained by considering the microcrack development in the cement paste. A lattice fracture model is employed to simulate the microcracks. The primary results of the proposed model are presented and discussed in the present paper.

1. INTRODUCTION

The transport of aggressive chemical species through the pore network in cement-based materials is an important issue in service life analyses of infrastructures. Determining transport properties of cement paste requires a group of experimental tests, which is not always practical. Therefore, several analytical and numerical models can be found in the literature regarding the estimation of the transport properties of cement-based materials [1-12]. More reliable and productive models are those that deal with simulation of the cement paste microstructure. Developments in computer technology made it possible to study the transport phenomena in cement-based materials considering a more sophisticated microstructure.

Among different transport phenomena in cement-based materials, the present study deals with diffusion modelling. Diffusion is a macroscopically observed phenomenon due to mass concentration difference. Fick's 1st and 2nd laws provide the equations that govern the phenomenon. However, at the microscopic scale diffusion is the Brownian motion of the ionic particles. All the ionic particles suspended in a solution move randomly in space with an equal probability. The following Einstein–Smoluchowski equation expresses the relation

between the macroscopic definition of diffusion and the microscopic view of the random movement of ion particles:

$$\left\langle l^2 \right\rangle = 6D^{self} t \tag{1}$$

where t represents time, $\left\langle l^2 \right\rangle$ is the averaged square distance of all the random-walking ions moved during time t, and D^{self} is the self-diffusion coefficient. The factor of 6 is connected with the approximate nature of the derivation, i.e., a three-dimensional random walk with ions being permitted to jump in six directions (forward and backwards, up and down, left and right) [8]. The present study is trying to estimate the diffusion coefficient of a specific ion in a cement paste at the macroscopic scale, by using the statistical data from the numerical modelling of the ions' random movement at the microscopic scale, using Eq. (1).

The cement paste microstructure is simulated using HYMOSTRUC3D [13, 14]. Then, a lattice model is constructed on the simulated microstructure based on the newly lattice configuration proposed by the authors [15]. On the basis of Eq. (1), a random walk algorithm (RWA) is developed to simulate the random movement of ionic particles in the pore structure of the simulated microstructure. The diffusivity of cement paste is determined by comparing the random walk of walkers in the pore network of cement paste with that of walkers in a free space with no restrictions in movement in any direction in space. In order to determine the diffusivity in cracked cement paste, the constructed lattice model is subjected to a tensile loading, as discussed recently in [15]. Then, the RWA is applied for the obtained cracked microstructure at different stages of the cracking strain. The methodology of the proposed numerical model is described in this paper, and the primary results of the diffusion coefficient for sound and cracked cement paste are compared.

2. CEMENT PASTE MICROSTRUCTURE

In the present study the latest version of HYMOSTRUC3D software [14, 16], developed in the Materials & Environment Department at Delft University, is used for constructing the cement paste microstructure during hydration. This simulation is implemented in a cubic REV volume of the cement paste where the cement particles are modelled as spheres randomly distributed. The initial number and diameter of the particles are built in accordance with the Particle Size Distribution (PSD) curve, which was obtained by using Laser Diffraction Spectrometry (LDS).

The main cement hydration products are the Calcium-Silicate-Hydrate (C-S-H) and the Calcium Hydroxide (CH). C-S-H is formed as two layers of inner and outer products, which are the result of the inward and outward radial growing of the cement spheres. An example of the simulated microstructure of a cement paste at a degree of reaction of 0.65 is illustrated in Figure 1. Main phases of this cement, measured by X-Ray diffraction, are composed of 70% of C3S, 20% of C2S, 4% of C3A and 1% of C4AF (mass percentages). The other important parameters to be defined in HYMOSTRUC3D for modelling cement hydration are minimum and maximum size of the cement particles, REV size, temperature, *w/c*, and two reaction factors that control the speed and progress of hydration. For further details on fundamental aspects of the model parameters, the reader is addressed to the studies published by Van Breugel and by Guang Ye [10,20]. The hydration parameters are calibrated using the degree of hydration measured through isothermal calorimetry, performed for the same cement and *w/c* ratio. By giving a relevant set of hydration parameters to the model, a good estimation is

obtained regarding the degree of reaction for the three cement paste mixtures under study. A typical Portland cement clinker is considered for the modelling in the present study, with a *w/c* = 0.4.

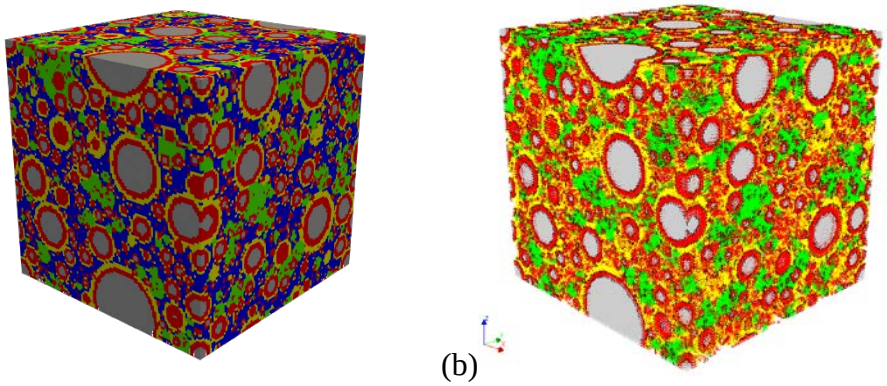

(a) (b)

Figure 1. 3D images of (a) the microstructure of a hydrated cement paste with a *w/c* = 0.4 and a degree of reaction of 0.65; (b) the lattice model constructed on the microstructure without pore phases (grey: unreacted cement grain, red: inner C-S-H, yellow: outer C-S-H, green: CH grain, blue: water/void)

3. CONSTRUCTION OF THE LATTICE MICROSTRUCTURE

The simulated microstructure – a REV with dimensions 100×100×100μm^3 – is initially discretized into small 1.0×1.0×1.0μm^3 voxels. A 3D lattice is constructed by means of individual unit cells, as shown in Figure 2a. It includes two types of nodes (middle and corner) and beams. The corner nodes are connected by regular lattice beams (l_1 = 1.0μm), whereas the middle and corner nodes are linked with diagonal beams ($l_2 = \sqrt{3}/2 l_1$, see Figure 2a). Therefore, each unit cell includes 8 diagonal and 10 regular lattice beams.

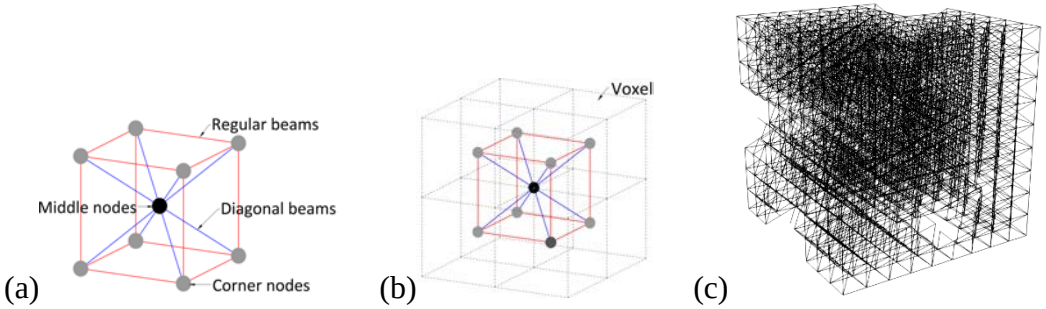

(a) (b) (c)

Figure 2. (a) Construction of the lattice unit cell based on truncated octahedral; (b) positioning of the lattice unit cell on the discretized REV voxels; (c) an example of a lattice construction excluding the pore nodes

To construct the 3D lattice model, the lattice unit cell is located in the discretized microstructure obtained from HYMOSTRUC3D, in the way depicted in Figure 2b. By adopting the same size for each lattice unit cell as the one of each voxel (i.e., 1.0μm), the corner nodes are precisely located in the centre of the 8 neighbouring voxels (see dotted cubes

in Figure 2b), and the middle node is placed at the vertices of the cubic voxel (see darker node in Figure 2b). By filling all the voxels with the lattice unit cells (excluding the water and void voxels), the whole 3D lattice model is constructed (see an example in Figure 2c).

4. MECHANICAL MODEL

In order to analyse the diffusivity of ionic particles in a cracked microstructure, a coupled mechanical-transport analysis is required. For this purpose, the lattice model constructed from the microstructure, as explained in Section 3, must be initially subjected to an incremental tensile loading configuration to obtain a damaged microstructure. The cracked microstructure at each stage of loading is then imported to the diffusivity numerical model. This section explains this mechanical model for obtaining the cracked lattice microstructure of a cement paste.

4.1. Model configurations

The constructed lattice model is imported to DIANA FEA computer software (released version 10.1), which is the numerical solver chosen in the present study. Note that for the sake of decreasing the number of finite elements (FE), the lattice beams and nodes corresponding to the pore phases are not considered in the construction of the lattice. Therefore, only the solid part of the microstructure (excluding the porosity) is imported to DIANA. The configuration of a uniaxial tensile test is arranged for the REV lattice microstructure by fixing all the nodes on the bottom surface of the specimen and imposing an incremental uniform surface displacement on the top surface.

The Class-I FE beam available in DIANA FEA is assigned for both the diagonal and regular lattice beams. Class-I FE beam is a two-nodded straight element based on the Timoshenko theory [17, 18], which has 12 degrees of freedom (D.O.F.): 3 displacements and 3 rotations at each extremity [19].

Mechanical properties of the regular beams are defined in accordance with the location of the nodal extremities. If the nodes are positioned in the same phase (two voxels with the same material), the beam has the mechanical properties of that phase; if not, an interface beam is considered between the two connected phases. On the other hand, the mechanical properties of the diagonal beams are defined only based on the properties of the middle node. This means that none of these beams counted as interfaces. For more details about the definition of the beam geometry and configurations, the reader is referred to the recent publication from the authors in [15]. Some mechanical properties of the cement hydration phases used in the mechanical modelling are provided in Table 1.

Table 1. Mechanical properties of material phases used in the lattice mechanical model

Cement hydration product	**Young's modulus (E)**	**Poisson's ratio (υ)**	**Tensile strength (f_{ct})**
	(GPa)	(-)	(MPa)
Unreacted cement	137	0.3	1.5
Inner C-S-H	29	0.3	0.25
Outer C-S-H	18	0.3	0.20
CH	35	0.3	0.30
Interfaces	Calculated using the classical Hashin-Shtrikman bounds method [15]		

Both regular and diagonal beams are assumed as cylindrical, with a constant circular cross-

section. Lengths l_1 for regular beams and l_2 for diagonal beams can be directly calculated from the coordinates at their nodal extremities. In the proposed regular model these values are constant and given by:

$$l_1 = l,\ l_2 = \left(\sqrt{3}/2\right)l \tag{2}$$

where l is the length of the voxels, adopted as 1.0μm in this study. The calculation of diameters d_1 and d_2, respectively, for the regular and diagonal beams is not straightforward. According to the calibration strategy detailed by the authors in [15], the geometrical data for the lattice beams are $d_1/l_1 = 0.9$ and $d_2/l_2 = 0.75$, respectively, for the regular and diagonal beams.

The Total Strain Based Crack Model available in the DIANA FEA software is assigned for mechanical behaviour of all the beams. In this model, a brittle behaviour is considered in tension, while the compressive behaviour is assumed linear elastic. When the principle tensile strain reaches the cracking strain (i.e., f_{ct}/E), the beam cracks and the stress drops to zero. Additionally, no shear stress is considered after cracking, by adopting a null value for the shear retention factor [19]. In fact, by reaching the cracking strain at each FE, this condition is similar to the removal of the beam from the model.

4.2. Stress-strain response of the microstructure under tensile loading

The constructed lattice model includes about 7 million lattice beams exclusive of the elements represented by the pore phases. Such large number of elements in a mechanical model for a nonlinear analysis is not practical to be run in a personal desk computer. Even though it can run on a computer cluster, it needs to allocate too much memory, and the analysis takes several days to be finished. Therefore, it is more practical to divide the model into smaller submodels. Then, an averaging strategy is followed to obtain the final stress-strain response from the submodels. For this purpose, the whole lattice microstructure is divided into 8 cubes, each with the dimensions of 50×50×50μm^3, as shown in Figure 3.

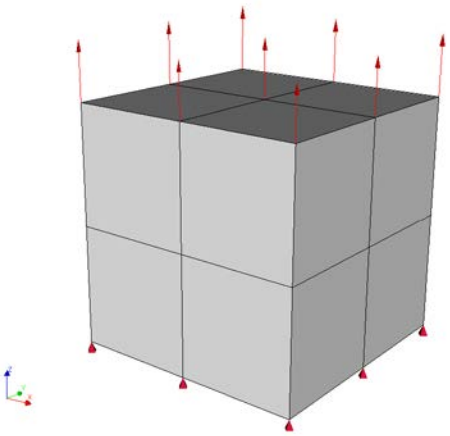

Figure 3. Subdivision of the REV microstructure into 8 cubes for the nonlinear analysis

By running a nonlinear analysis on each cube, 8 stress-strain responses are obtained, as plotted in Figure 4a. The total response of the original REV is estimated by calculating the average curve from these 8 responses, as plotted in Figure 4b. The obtained cracked lattice at different steps of analysis for all the 8 cubes are assembled to obtain the whole cracked REV,

which is then exported to the diffusivity analysis. Five steps of analysis (Steps 1 to 5) are selected for this purpose, which correspond to averaged total tensile strains of 0.002‰, 0.004‰, 0.006‰, 0.01‰ and 0.02‰. Examples of the obtained cracked lattice microstructures for the first cube at Steps 2 to 5 are shown in Figure 5. Note that Step 1 of analysis is in the linear elastic phase, with almost no cracks for all the cubes.

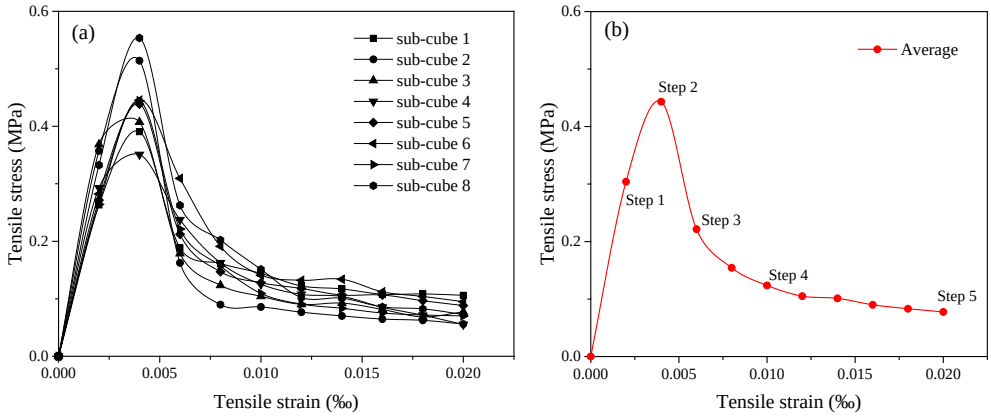

(a) (b)

Figure 4. Tensile stress *vs*. strain curves of the lattice microstructure: (a) for each cube, (b) the average curve

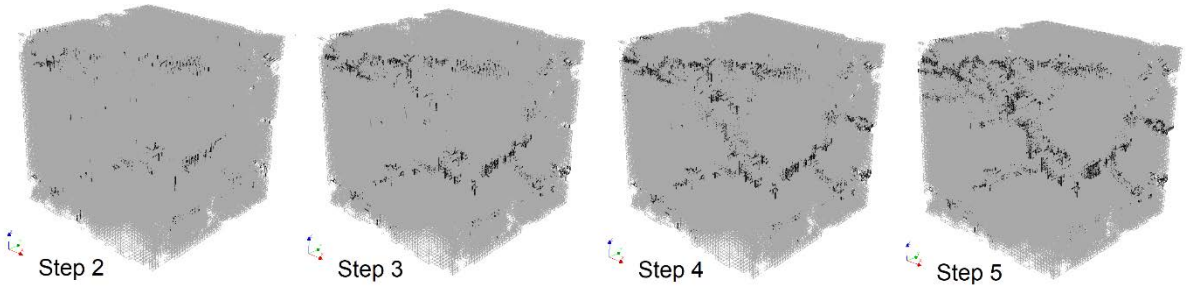

Figure 5. Illustration of the cracked lattice microstructure at 4 steps of the mechanical nonlinear analysis for one cube (black colour represents cracked lattice beams)

5. RANDOM WALK ALGORITHM

Diffusion can be accounted as a statistical result of ions random movements in a medium. Based on this definition, a random walk algorithm (RWA) is employed to numerically model the diffusion process [20, 21]. By comparing the data from random movements of walkers in the pore medium of a cement paste microstructure with that of walkers in a free space without any restraint, the diffusivity of cement paste for ion *i* is related to its self-diffusion coefficient defined by Eq. (1) [8]:

$$\frac{D_i^{cp}}{D_i^0} = \varphi \frac{D_{cp}^{self}}{D_{free}^{self}} = \varphi \frac{\left\langle l_{cp}^2 / t \right\rangle}{\left\langle l_{free}^2 / t \right\rangle} \tag{3}$$

where φ is the total porosity of the cement paste, which is computed by HYMOSTRUC3D. The ratio D_i^{cp} / D_i^0 is called relative diffusivity for the specific ion *i* [22]. D_i^{cp} is the diffusion coefficient of ion *i* of the cement paste, and D_i^0 is the diffusion coefficient of that ion in the

pore solution (as the reference solution) at a given temperature, which can be obtained from experiments. For instance, the diffusivity of chlorides in free water (reference solution for saturated microstructure in water) at room temperature is $D_{cl}^{0} = 2.03\times10^{-9}\,\mathrm{m^2/s}$, based on the study reported by Pivonka et al. in 2004 [23]. D_{cp}^{self} is the self-diffusion coefficient of the cement paste microstructure, and D_{free}^{self} is the self-diffusion coefficient in free space, both being independent of the ion type. $\left\langle l_{cp}^{2}/t \right\rangle$ and $\left\langle l_{free}^{2}/t \right\rangle$ are the averaged squared distances of all the random walkers in, respectively, the pore network of the cement paste and in a free 3D space. Therefore, by determining these two values the relative diffusivity of an ionic particle in the cement paste can be estimated.

It is worth noting that the self-diffusion coefficient D^{self} and the diffusion coefficient D_i are two concepts that are defined in different ways. The former describes the travelling of diffusing particles due to thermal motion in a chemically uniform environment, while the latter describes the diffusion process driven by a spatial concentration gradient [10]. These two are related to each other by Eq. (3).

5.1. RWA in a sound paste

In case of RWA in a sound cement paste (no cracks), each lattice beam is a moving path between the two connected nodes. If the two nodes correspond to the two permeable material phases, the diffusion of ions is allowed in that beam. Otherwise, the ions are restricted to move through the beam. In the present study, the pores (water or void) are the only material phases where diffusion is allowed. All the solid material phases, including unreacted cement, inner and outer C-S-H and CH are assumed impenetrable materials. This assumption may not be accurate in case of the outer C-S-H, which comprises a significant amount of gel pores. However, this effect is neglected in the present work, as the focus is put only on the explanation of the methodology and on presenting some preliminary results.

1. In RWA walkers (represented by ionic particles) are randomly located at the lattice nodes that correspond to the pore phases. The located walker is permitted to move through the beam that connects to a pore neighbour node. The same probability of movement is considered for all directions, at each time-step. Each step is assumed to be independent of the previous walk.

Considering the regular lattice beams with a length l_1=1.0, the time required for the walker to pass through this beam as Δt, and assuming that the walker can move by only one direction at each time-step, the self-diffusion coefficient becomes ion-type-independent and unit-less. This coefficient can be computed based on a sufficiently long travelling time t (large number of time-steps):

$$D_{cp}^{self} = \frac{1}{6}\left\langle \frac{{l_{cp}}^{2}(t_i)}{t_i} \right\rangle \tag{4}$$

and a sufficiently large number of walkers N_w, averaging as follows

$$\left\langle \frac{{l_{cp}}^{2}(t_i)}{t_i} \right\rangle = \frac{1}{N_w}\sum_{i=1}^{N_w}\left[\frac{\left(x_i^t - x_i^0\right)^2 + \left(y_i^t - y_i^0\right)^2 + \left(z_i^t - z_i^0\right)^2}{t_i} \right] \tag{5}$$

where t_i, $\left(x_i^0, y_i^0, z_i^0\right)$ and $\left(x_i^t, y_i^t, z_i^t\right)$ are, respectively, the final travelling time, and the initial

and the end positions of the i^{th} walker. Note that if the randomly selected direction corresponds to an impenetrable lattice beam, the time increases by a unit time-step but no movement is recorded. Additionally, since the length of the diagonal beams is smaller than the one of the regular beams ($l_2 = \sqrt{3}/2 l_1$), the time required for the walker to pass through the diagonal beams should be less than Δt. Hence, an equivalent time-step Δt_{eq} is introduced in the simulation, being $\Delta t_{eq} = \sqrt{3}/2\,\Delta t$ for diagonal beams and $\Delta t_{eq} = \Delta t$ for regular beams. The final travelling time is computed by summation of all the equivalent time-steps at each movement for the i^{th} walker. Figure 6 illustrates the flowchart of the RWA in a lattice microstructure for a walker. The algorithm is repeated for the desired number of walkers N_w.

An analysis region with dimensions 500×500×500μm^3 is considered for the RWA model. The region includes the original REV locating at the centre, which is periodically repeated in the three orthogonal directions. The starting location of the walker is somewhere in the middle of the centred REV, being allowed to move randomly throughout the region. The region of analysis, and an example of a walker's path in either a cement paste microstructure and in a free space region are shown in Figure 7. For the same number of time-steps, a walker in a free region reaches the boundary, while a walker in the cement paste microstructure remains inside the region. In the RWA simulation, if the walker reaches the boundary of the region, the analysis ends. For this reason, the region is chosen large enough, so the random walker stays inside the region during the travelling time *t*. In fact, selecting the size of the region depends on the number of time-steps.

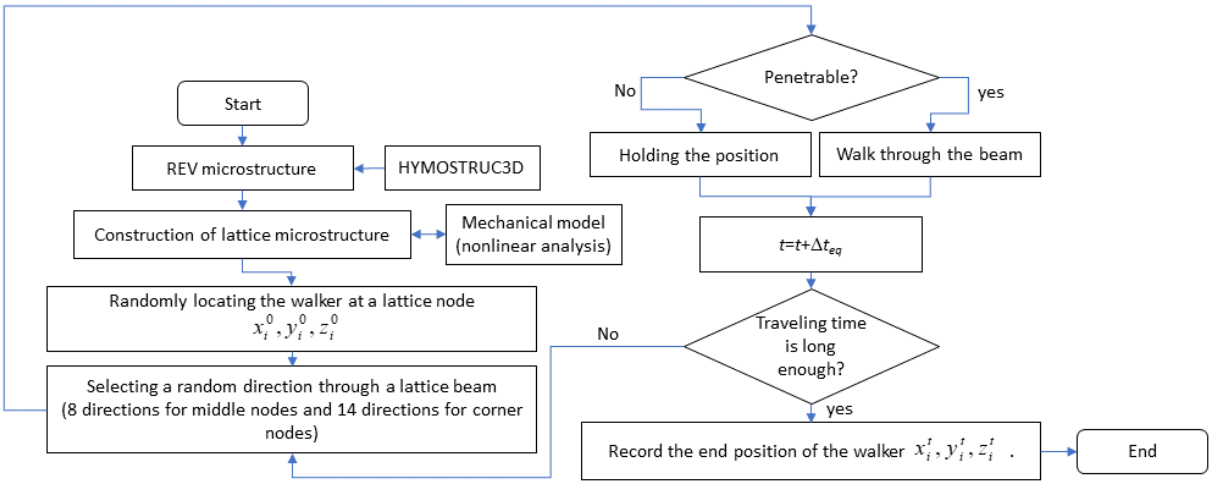

Figure 6. Flowchart of the RWA in a lattice microstructure of the cement paste

5.2. RWA in a cracked microstructure

In case of RWA in a cracked microstructure, the lattice is imported from the mechanical model (see Section 4). The imported cracked lattice does not include the beams represented by the pore phases in the original sound lattice model. Therefore, in case of cracked microstructure, the cracked lattice beams obtained from the mechanical model must be added to the original sound model. In fact, the cracked beams are the additional moving paths in the cracked microstructure. The principle of RWA in the cracked lattice microstructure is similar to the one in a sound microstructure. The same algorithm shown in Figure 6 is thus used,

being the lattice microstructure replaced by the cracked one in the mechanical model. Note that the total porosity φ given by HYMOSTRUC3D is valid for the sound cement paste. In case of the cracked cement paste, the total porosity is changed due to the cracking. The percentage of the cracked lattice beams should be added to the total porosity obtained from HYMOSTRUC3D.

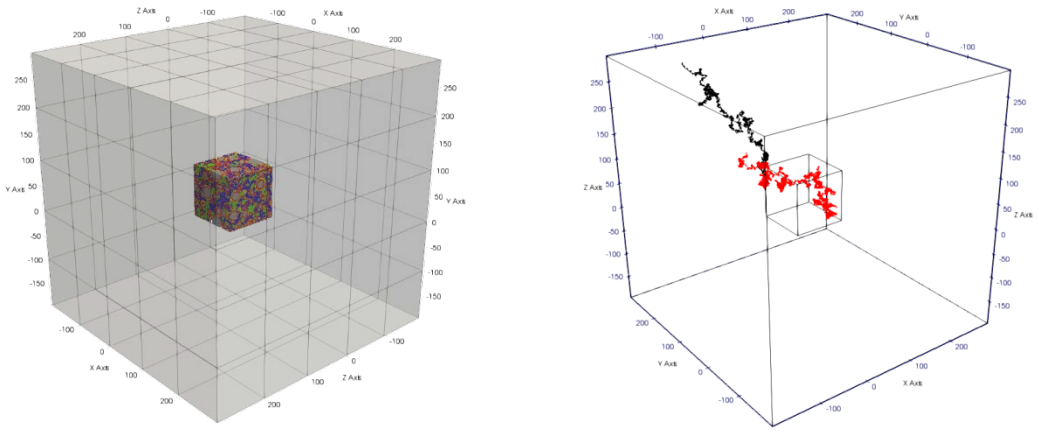

Figure 7. The cubic region of an RWA simulation (dimensions 500×500×500μm^3) and moving paths of a walker in the cement paste microstructure (red colour) and in the free space (black colour)

5.3. RWA in the free space

The principle of the RWA in the free space (or reference pore solution of cement paste) is similar to the one in sound lattice microstructure. In this case, all the lattice nodes are considered as pore material phases (water or void). Therefore, the walkers are allowed to diffuse through all the lattice beams. Based on this configuration, the value obtained from Eq. (4) is the self-diffusion coefficient in the free space, D_{free}^{self}.

5.4. Reliability of the results from RWA

To determine a reliable value for the self-diffusion coefficient, the number of walkers N_w and the travelling time t must be sufficiently large. To verify the reliability of the results from RWA, the influence of changing N_w and t is evaluated on the ratio $\left\langle l_{cp}^2/t\right\rangle/\left\langle l_{free}^2/t\right\rangle$. For this purpose, two parametric analyses are implemented:

1) the number of time-steps is kept constant ($t = 5\times10^4$), while N_w varies from 1 to 10^6;
2) the number of walkers is kept constant ($N_w = 10^3$), while the number of time-steps varies from 1 to 7×10^5.

The results of these two analyses are plotted in Figure 8. In the first analysis, the ratio $D_{cp}^{self}/D_{free}^{self}$ converges to a constant value with the increasing number of walkers, and the curve shows a smoother trend when N_w is larger than 10^3. The results are highly scattered for N_w less than 100. In the second analysis, with $N_w = 10^3$, results are acceptable even for the lower number of time-steps. However, the ratio $D_{cp}^{self}/D_{free}^{self}$ converges to a constant value only when the number of time-steps is larger than about 5×10^4. In the following simulations

in this paper $N_w = 10^3$ and the number of time-steps is taken as 5×10^4.

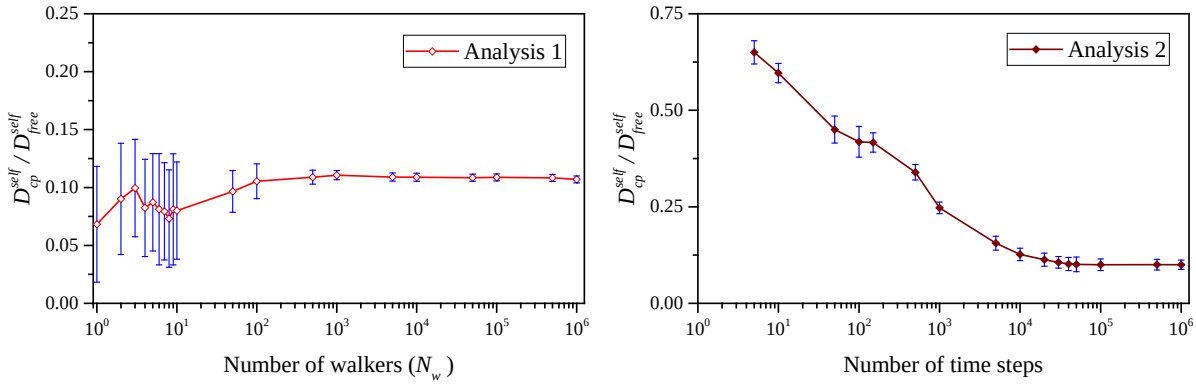

Figure 8. Influence of the number of walkers and of the number of time-steps in RWA simulations of the self-diffusivity coefficient

6. DIFFUSIVITY OF SOUND AND CRACKED CEMENT PASTES

The results from the RWA for sound (Step 1) and cracked microstructure of cement pastes (Steps 2 to 5) in terms of the self-diffusion coefficient are shown in Figure 9a: the ratio $D_{cp}^{self} / D_{free}^{self}$ increases by increasing the total tensile strain in REV, which represents the development of the microcracks in the cement paste.

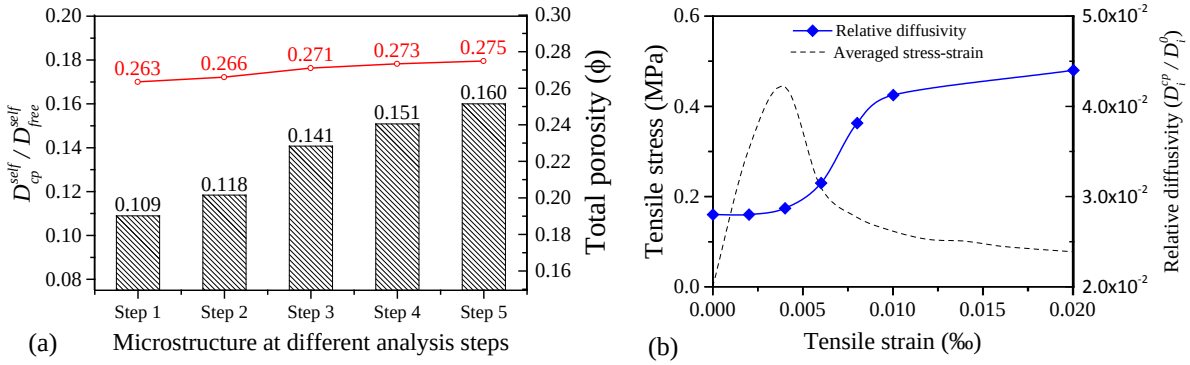

Figure 9. (a) Self-diffusivity coefficient from RWA in sound and in cracked cement paste microstructure; (b) change in relative diffusivity by increasing the cracked tensile strain in REV

The change in the total porosity is also plotted in Figure 9b, as shown in the secondary vertical axis. The porosity, which shows a slight change by microcracks development, is used in Eq. (3) to calculate the relative diffusivity coefficient for the cracked cement paste. In this figure, the ionic relative diffusivity of the cement paste is plotted versus the total tensile strain in REV. After the peak in the tensile stress-strain curve of the REV, the relative diffusivity increases rapidly until a certain cracking strain. After this point, the ratio remains almost constant with no significant increasing rate.

7. SUMMARY AND CONCLUSIONS

A 3D numerical modelling strategy was proposed in the present study to estimate the ionic

relative diffusivity in both sound and cracked cement paste. The model used the REV of cement paste microstructure provided by the HYMOSTRUC3D software. First, a 3D lattice model, recently proposed by the authors, was constructed based on the HYMOSTRUC3D microstructure. Then, a methodology was adopted to simulate the mechanical tensile behaviour of the lattice cement paste microstructure under uniaxial tensile loading. By using this mechanical model, the stress-strain response of the microstructure under tensile loading, as well as the microcracking development, were obtained. Both sound and cracked microstructures (at different steps of tensile loading) were imported to the random walk algorithm (RWA), to compute the self-diffusivity coefficient of the cement paste. Considering the physical laws, the computed self-diffusivity could be transformed into the steady state ionic diffusion coefficient knowing the pore solution properties. In the present study, the model accounted only for large capillary pores as transport pathways for ionic particles. However, the model can be easily extended to account for smaller capillary pores, using the nanostructure of C-S-H layers through a multi-scaling simulation scheme. A summary of the model methodology has been described and some primary results of the model have been demonstrated. The model showed success in computing the effect of microcracking on increasing the cement paste diffusion coefficient. The tendency of diffusivity to increase was evaluated versus the total tensile strain in the REV microstructure. This data will be useful for a multiscale modelling strategy in future studies to determine the diffusion properties of the concrete material at a macro scale.

8. ACKNOWLEDGEMENTS

This work was supported by projects POCI-01-0145-FEDER-007457 (CONSTRUCT - Institute of R&D in Structures and Construction) and POCI-01-0145-FEDER-007633 (ISISE - Institute for Sustainability and Innovation in Structural Engineering), funded by FEDER through COMPETE2020 - Programa Operacional Competitividade e Internacionalização and by national funds through FCT - Fundação para a Ciência e a Tecnologia. FCT and FEDER (COMPETE2020) are also acknowledged for funding the research project PTDC/ECM-EST/1056/2014 (POCI-01-0145-FEDER-016841). The first author is also thankful for the grant with reference number SFRH/BPD/114754/2016 funded by FCT.

9. REFERENCES

[1] Luc Dormieux and Eric Lemarchand, *Homogenization approach of advection and diffusion in cracked porous material*. Journal of engineering mechanics, 2001. **127**(12): p. 1267-1274.

[2] Sabine Caré, *Influence of aggregates on chloride diffusion coefficient into mortar*. Cement and Concrete Research, 2003. **33**(7): p. 1021-1028.

[3] Jacques Marchand, Ivan Odler, and Jan P Skalny, *Sulfate attack on concrete*. 2003: CRC Press.

[4] Sabine Caré and E Hervé, *Application of a n-phase model to the diffusion coefficient of chloride in mortar*. Transport in Porous Media, 2004. **56**(2): p. 119-135.

[5] S. Kamali-Bernard and F. Bernard, *Effect of tensile cracking on diffusivity of mortar: 3D numerical modelling.* Computational Materials Science, 2009. **47**(1): p. 178-185.

[6] S Kamali-Bernard, F Bernard, and W Prince, *Computer modelling of tritiated water diffusion test for cement based materials.* Computational Materials Science, 2009. **45**(2): p. 528-535.

[7] Mingzhong Zhang, Guang Ye, and Klaas Van Breugel, *Microstructure-based modeling of water diffusivity in cement paste.* Construction and Building Materials, 2011. **25**(4): p. 2046-2052.

[8] Lin Liu, Wei Sun, Guang Ye, Huisu Chen, and Zhiwei Qian, *Estimation of the ionic diffusivity of virtual cement paste by random walk algorithm.* Construction and Building Materials, 2012. **28**(1): p. 405-413.
[9] Qing-feng Liu, Jian Yang, Jin Xia, Dave Easterbrook, Long-yuan Li, and Xian-Yang Lu, *A numerical study on chloride migration in cracked concrete using multi-component ionic transport models.* Computational Materials Science, 2015. **99**: p. 396-416.
[10] Hongyan Ma, Dongshuai Hou, and Zongjin Li, *Two-scale modeling of transport properties of cement paste: Formation factor, electrical conductivity and chloride diffusivity.* Computational Materials Science, 2015. **110**: p. 270-280.
[11] S. D. Abyaneh, H. S. Wong, and N. R. Buenfeld, *Simulating the effect of microcracks on the diffusivity and permeability of concrete using a three-dimensional model.* Computational Materials Science, 2016. **119**: p. 130-143.
[12] N. Seigneur, E. L'Hôpital, A. Dauzères, J. Sammaljärvi, M. Voutilainen, P. E. Labeau, A. Dubus, and V. Detilleux, *Transport properties evolution of cement model system under degradation - Incorporation of a pore-scale approach into reactive transport modelling.* Physics and Chemistry of the Earth, Parts A/B/C, 2017. **99**: p. 95-109.
[13] Klaas Van Breugel, *Numerical simulation of hydration and microstructural development in hardening cement-based materials:(II) applications.* Cement and Concrete Research, 1995. **25**(3): p. 522-530.
[14] Guang Ye, *Experimental study and numerical simulation of the development of the microstructure and permeability of cementitious materials*. 2003: PhD Thesis. TU Delft, Delft University of Technology.
[15] Hadi Mazaheripour, Rui Faria, Guang Ye, Erik Schlangen, José Granja, and Miguel Azenha, *Microstructure-Based Prediction of the Elastic Behaviour of Hydrating Cement Pastes.* Applied Sciences, 2018. **8**(3): p. 442.
[16] Klaas Van Breugel, *Simulation of hydration and formation of structure in hardening cement-based materials*. 1991: TU Delft, Delft University of Technology.
[17] S Timoshenko and JN Goodier, *Theory of elasticity. 1951.* New York. **412**: p. 108.
[18] B. L. Karihaloo, P. F. Shao, and Q. Z. Xiao, *Lattice modelling of the failure of particle composites.* Engineering Fracture Mechanics, 2003. **70**(17): p. 2385-2406.
[19] *Element Library*, in *DIANA-10.1 User's Manual*, J. Manie, Editor., DIANA FEA.
[20] Ahmed F. Ghoniem and Frederick S. Sherman, *Grid-free simulation of diffusion using random walk methods.* Journal of Computational Physics, 1985. **61**(1): p. 1-37.
[21] Călin Vamoş, Nicolae Suciu, and Harry Vereecken, *Generalized random walk algorithm for the numerical modeling of complex diffusion processes.* Journal of Computational Physics, 2003. **186**(2): p. 527-544.
[22] E. J. Garboczi and D. P. Bentz, *Computer simulation of the diffusivity of cement-based materials.* Journal of Materials Science, 1992. **27**(8): p. 2083-2092.
[23] Peter Pivonka, Christian Hellmich, and David Smith, *Microscopic effects on chloride diffusivity of cement pastes—a scale-transition analysis.* Cement and Concrete Research, 2004. **34**(12): p. 2251-2260.